analytical chemistry

pubs.acs.org/ac Article

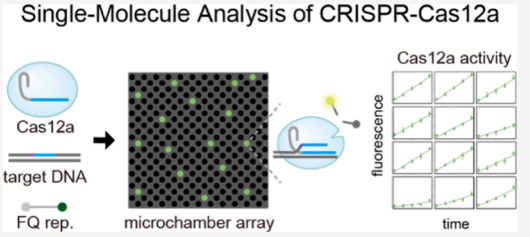
Single-Molecule Characterization of CRISPR–Cas12a for Amplification-Free Genetic Testing

Hajime Shinoda,* Asami Makino, Mami Yoshimura, Tatsuya Iida, Daisuke Yamazaki, Noriko Minagawa, Yasushi Kogo, Takako Sano, Michio Jinnai, Takayuki Hishiki, Hitomi Ohya, Hiroshi Nishimasu, and Rikiya Watanabe*

Cite This: https://doi.org/10.1021/acs.analchem.6c00936 Read Online

ACCESS | Metrics & More | Article Recommendations | Supporting Information

ABSTRACT: CRISPR–Cas-based genetic testing has gained considerable attention for rapid and accurate diagnosis of infectious and genetic diseases. Cas12a, an RNA-guided nuclease that targets DNA, has been widely applied for DNA detection; however, its detailed enzymatic properties have not been fully elucidated. Here, we performed a systematic single-molecule analysis of Cas12a using microchamber arrays to biophysically characterize its catalytic behavior including protospacer adjacent motif (PAM) specificity, mismatch tolerance, and reaction kinetics and to evaluate the feasibility and inherent challenges of amplification-free DNA detection. Cas12a exhibited high activation efficiency toward target DNA, demonstrating the feasibility of amplification-free DNA detection with a detection limit of 104 aM within 15 min. However, Cas12a also exhibited substantial nonspecific cross-reactivity with genome-length targets, particularly mammalian genomic DNA, identifying off-target activation as a major challenge for reliable diagnostic application. Together, these findings provide a quantitative biophysical characterization of Cas12a-based amplification-free DNA detection and highlight the need to improve its target specificity for future reliable application of Cas12a in amplification-free molecular diagnostics.



Downloaded via SHENZHEN UNIV on July 6, 2026 at 02:02:08 (UTC).
See https://pubs.acs.org/sharingguidelines for options on how to legitimately share published articles.

INTRODUCTION

The recent pandemic of viral infections has highlighted the urgent need for rapid, accurate, and accessible genetic testing technologies.[1,2] Conventional genetic assays such as PCR provide high sensitivity and specificity but require time-consuming amplification steps and sophisticated instrumentation, limiting their suitability for point-of-care applications. In contrast, antigen tests enable faster and simpler screening but often lack sufficient analytical performance for definitive diagnosis.

CRISPR–Cas systems have recently emerged as a powerful alternative platform for molecular diagnostics.[3−7] These RNA-guided nucleases, derived from the bacterial adaptive immune system, recognize and cleave target nucleic acids. Among them, Cas12 and Cas13 have been utilized for nucleic acid detection through their programmable target recognition and collateral cleavage (*trans*-cleavage), producing fluorescence signals in response to specific nucleic acid sequences.[5,8] When combined with amplification reactions such as PCR, CRISPR-based assays can detect nucleic acids within approximately 30 min with high sensitivity. In parallel, the development of digital bioanalysis has expanded the potential of CRISPR diagnostics toward direct, amplification-free detection at the single-molecule level.[9−14]

Cas13, which targets RNA, exhibits high *trans*-cleavage activity, making it advantageous for rapid RNA detection.[7,12,15] Building on this property, we previously developed an amplification-free RNA detection platform, SATORI, which achieved single-molecule quantification within 10 min.[15,16] For DNA detection, Cas12a has been widely used, and various optimization strategies including PAM engineering,[17] mismatch tolerance characterization,[17] and crRNA design[18] have been explored, primarily in bulk-format amplification-coupled assays. However, the biophysical properties of Cas12a at the single-molecule level remain incompletely characterized, and the feasibility of Cas12a for amplification-free DNA detection has not been systematically evaluated.

In this study, we extend the SATORI platform to DNA detection by performing a systematic single-molecule analysis of Cas12a. Rather than aiming to establish a superior amplification-free DNA detection methodology, our goals are to (i) biophysically characterize the catalytic behavior of Cas12a including PAM specificity and mismatch tolerance at the single-molecule level, (ii) re-examine previously reported optimization strategies under single-molecule conditions, and (iii) evaluate the feasibility of amplification-free single molecule DNA detection with Cas12a. We demonstrated

Received: February 5, 2026
Revised: June 11, 2026
Accepted: June 24, 2026

© XXXX American Chemical Society

https://doi.org/10.1021/acs.analchem.6c00936
Anal. Chem. XXXX, XXX, XXX−XXX

attomolar-sensitivity detection of target DNA within ~15 min using Cas12a in an amplification-free, single-molecule format. However, Cas12a also exhibited nonspecific cross-reactivity with long nontarget sequences (e.g., genomic DNA from human and mouse), identifying off-target activation as a major challenge for reliable diagnostic applications. Together, these findings provide a quantitative biophysical foundation for Cas12a-based amplification-free DNA detection and highlight the engineering requirements for its future translation into molecular diagnostics.

MATERIALS AND METHODS

Fabrication of CD-Based Microchamber Array Devices

The original mold was prepared by photolithography using a 3D drawing system (DWL66+, Heidelberg Instruments), and a Ni replica was fabricated by electrocasting. The CD-based microchamber device containing ~10^8 microchambers (V = ~30 fL, Φ = 3.5 μm, h = 3.5 μm) was fabricated from polycarbonate resin using a molding machine with the above mold (SD40ER, Sumitomo). A UV-curable acrylic resin (5 × 649H, Chemitech) and dispensing robot (SHOTmini 200SX, Musashi Engineering) were used to fabricate a ring-shaped enclosure with a diameter of 7 mm on the CD.

Preparation of Cas12a

pET-en*Lb*Cas12a plasmid was prepared by introducing D156R/G532R/K538R mutations into pET-*Lb*Cas12a plasmid. For expression of *Lb*Cas12a or en*Lb*Cas12a, *Escherichia coli* Rosetta 2 (DE3) was transformed with the pET-*Lb*Cas12a and pET-en*Lb*Cas12a plasmids, and the cells were cultured in 2.5 L of LB medium containing kanamycin. When the OD600 values reached 0.6−1.0, the cells were cooled on ice for 10 min, and were further cultured at 20 °C for 20 h with 0.1 mM IPTG. Bacterial cells were collected by centrifugation, suspended in 40 mL buffer A (20 mM Tris-HCl (pH 8.0), 1 M NaCl, 20 mM imidazole, 3 mM β-mercaptoethanol (ME) and 1 mM phenylmethylsulfonyl fluoride), and disrupted by sonication (Q500, QSONICA). After centrifugation at 15,000 rpm for 20 min, the supernatant was incubated with Ni-NTA agarose (Qiagen) at 4 °C for 1 h. The mixture was subsequently transferred to an Econo column (Bio-Rad). The resin was washed with buffer B (20 mM Tris-HCl (pH 8.0), 0.3 M NaCl, 20 mM imidazole and 3 mM ME), and the protein was eluted with buffer C (20 mM Tris-HCl (pH 8.0), 0.3 M NaCl, 300 mM imidazole and 3 mM ME). The protein was then loaded onto a HiTrap SP HP column (Cytiva) equilibrated with buffer D (50 mM HEPES-KOH (pH 7.5), 0.3 M NaCl and 0.5 mM Tris(2-carboxyethyl)phosphine (TCEP)). The protein was eluted using a linear gradient from 0.3 to 2.0 M NaCl over 7 column volumes. The protein was further purified by size exclusion chromatography (Enrich SEC 650, Bio-Rad) with buffer E (50 mM HEPES-KOH (pH 7.5), 0.5 M NaCl and 0.5 mM TCEP).

RNA Preparation

FAM−TTATT−IBFQ reporter (FQ reporter) and crRNAs were purchased from IDT and Hokkaido System Science Co. (Table S1). Target DNA fragments (Table S2) were prepared by PCR reaction with KOD+ polymerase kit (Toyobo) and primer sets (Table S3), and purified by agarose-gel electrophoresis and a kit. The RNA and DNA concentrations were determined from A_{260} values using a NanoDrop spectrophotometer (Thermo Fisher Scientific). Human genome (G1521, Promega), mouse genome (G3091, Promega) and *E. coli* genome (MBD0013, Sigma-Aldrich) were used to check cross-reactivity.

Mpox Virus (MPXV) Genome Preparation

MPXV were propagated in VeroE6 or Vero cells with E-MEM medium (051-07615, FUJIFILM Wako) containing 2% fetal bovine serum (FBS) and 1% penicillin/streptomycin at 37 °C with 5% CO_2. Viral supernatants were collected 7 days after infection, and the viral DNA was purified using QIAamp DNA Mini Kit (51304, QIAGEN). The concentration of the MPXV genome was determined by qPCR with QuantiTect Probe PCR Kit (Qiagen), primers/probes, and reference genes (Table S4).

Automation Platform of the Single-Molecule Assay

The single-molecule assay was performed on an automated platform[15] that integrated a custom-built automatic dispensing system (BioTec) with a confocal fluorescence microscope (A1HD25, Nikon) equipped with a 20× objective (Nikon), 488 and 640 nm lasers, and a motorized XY scanning stage. A neodymium magnet (HXN10-10, Misumi) was mounted on the automated objective-lens turret of the microscope to concentrate magnetic beads into the CD-based microchamber device. A cylindrical aluminum block warmed by a lens heater (Tokai Hit) was attached to the chamber array device, or alternatively, a transparent indium tin oxide (ITO) glass heater with 1 mm thick was mounted on the device to maintain the microchamber array at a constant temperature.

Single-Molecule Assay without the Target-Capture Step

Cas12a−crRNA complexes were prepared by mixing 0.7 μL of Cas12a (20 μM), 1.4 μL of crRNA (2.5 μM) and 2.6 μL of buffer F (20 mM HEPES-KOH (pH 7.5), 150 mM KCl, 10 mM $MgCl_2$ and 50 μM Triton X-100), and incubating at 37 °C for 10 min. The mixture was then diluted with 4-fold volumes of the buffer F containing 15 μM FQ reporter and 75 μM Alexa Fluor 647 dye (Thermo Fisher Scientific). Target DNAs were prepared in buffer G (10 mM Tris-HCl (pH 9.0), 10 mM NaCl, 15 mM $MgCl_2$ and 50 μM Triton X-100). For amplification-free DNA detection assay on the automated platform, 20 μL of the Cas12a−crRNA mixture was combined with 100 μL of the target DNA solution. After 1 min of incubation, 105 μL of the mixture was dispensed onto a CD-based device and pipetted repeatedly for 1 min. Approximately 95 μL of the solution was then removed, and 50 μL of Fomblin oil was added at a rate of 5 μL/s to seal the microchambers. The excess solution and oil remaining on the CD were removed, and fluorescence tiling images were acquired after incubation. For the kinetics measurement of Cas12a, after the oil sealing, image acquisition was repeated at time interval of 2.5 min. The number of cleaved FQ reporters was calculated based on the calibration curve of the mean fluorescence intensity and the concentration of fluorescein-conjugated ssDNA (Figure S1).

Single-Molecule Assay with the Target-Capture Step

Biotinylated Cas12a was prepared by incubating Cas12a (20 μM) with NHS−$dPEG_2$−biotin (Quanta BioDesign) at molar ratios of approximately 1:1 for 1 h at room temperature. Cas12a−crRNA complexes were then prepared in the same manner as described above. The assay mixture for Cas12a was prepared in buffer F, containing 60−12.5 nM Cas12a−crRNA complexes, 12 μM FQ reporter, and 60 μM Alexa Fluor 647 carboxylic acid. Magnetic beads (Sera-Mag Streptavidin Binding Capacity (High), 30152105010150, Cytiva) were washed and resuspended in buffer H (10 mM Tris-HCl (pH 9.0), 10 mM NaCl, 15 mM $MgCl_2$, and 500 μM Triton X-100) at a final concentration of 0.5 mg/mL. For the amplification-free DNA detection assay with a target-capture step on the automated platform, 20 μL of the Cas12a mixture was combined with 100 μL of the target DNA solution, followed by the addition of 20 μL of the magnetic bead solution. After 3 min of incubation, 105 μL of the mixture was dispensed onto a CD-based device and pipetted for 10 s. A neodymium magnet (HXN10−10, Misumi) was positioned directly beneath the device via the automated objective-lens turret of the microscope. Of the 105 μL of solution on the CD device, 95 μL was removed, and 50 μL of Fomblin oil was subsequently added at a rate of 5 μL/s. Excess solution and oil remaining on the CD were removed, and fluorescence tiling images were acquired after incubation using a 20× objective lens.

For direct DNA detection from a biological matrix, 50 μL of the sample placed on a motorized magnet lift was mixed with 20 μL of biotinylated Cas12a−crRNA complexes (60−12.5 nM) in buffer F and 50 μL of buffer I (20 mM HEPES-KOH [pH 7.5], 150 mM KCl, 20 mM $MgCl_2$, × 1/50 RNase inhibitor [M0314, NEB] and 15 mM Triton X-100). After incubation for 1 min, the supernatant was removed using a motorized magnet lift, leaving behind the magnetic

https://doi.org/10.1021/acs.analchem.6c00936
Anal. Chem. XXXX, XXX, XXX−XXX

beads. Next, the magnetic beads were washed with 250 μL of buffer J (10 mM Tris-HCl [pH 9.0], 10 mM NaCl, 15 mM $MgCl_2$ and 500 μM Triton X-100) and resuspended in 110 μL of buffer G containing 2 μM FQ reporter, 10 μM Alexa Fluor 647 carboxylic acid and × 1/1000 RNase inhibitor. The mixture was sealed into the CD-based device in the same manner as described above, and fluorescence tiling images were acquired after incubation using a 20× objective lens.

Data Analysis

For single-molecule assay without target-capture step, the obtained green channel images (corresponding to FAM fluorescence) were analyzed using the NIS-Elements software (Nikon) with the Object Count command. The following parameters were applied: diameter 3−6 μm, circularity 0.6−1.0, and threshold 1,500, to identify positive chambers and extract region of interest (ROI) information. False positives were suppressed by excluding ROIs with a green/red (corresponding to Alexa Fluor 647 fluorescence) intensity ratio <2. This ratio-based filtering decreases false-positive signals arising from dust particles, which emit scattering-derived signals in both the green and red channels, whereas genuine Cas-derived signals are observed predominantly in the green channel owing to FQ-reporter cleavage.[15]

For the single-molecule assay with the target-capture step, green channel images were analyzed using the parameters: diameter 3−6 μm, circularity 0.6−1.0, and threshold 1,500. False positives were suppressed by excluding ROIs with a green/red intensity ratio <2. To further eliminate false positives, the number of chambers detected 7.5 min after oil sealing was subtracted from the number detected 12.5 min after oil sealing.

The analytical limit of detection (LoD) was defined as follows. The number of positive chambers obtained with different concentrations of the tgDNA was fitted to a linear function. The mean +3 SD value for the number of positive chambers obtained without tgDNA was determined, and the crossing point of the linear fitting and the mean +3 SD was then determined. The concentration corresponding to the crossing point was defined as the LoD value.

To evaluate the *trans*-cleavage activity of Cas12a, the acquired fluorescence images were analyzed using ImageJ (Fiji) or NIS-Elements (Nikon). Briefly, ROIs were defined on the final frame of each time-lapse image to identify fluorescence-positive chambers, and the maximum fluorescence intensity within each chamber was tracked throughout the time series to obtain fluorescence-intensity trajectories. Based on calibration curve between fluorescence intensity and FAM concentration (Figure S1), the *trans*-cleavage rate was calculated.

RESULTS AND DISCUSSION

Single-Molecule Analysis of CRISPR−Cas12a

Cas12a forms a binary complex with CRISPR RNA (crRNA) that recognizes and binds double-stranded target DNA (tgDNA) complementary to the crRNA spacer sequence. Upon target binding, Cas12a undergoes a conformational change that activates its RuvC nuclease domain, enabling cleavage of the tgDNA (*cis*-cleavage) and collateral degradation of nontarget single-stranded DNAs in solution (*trans*-cleavage).[5]

We characterized Cas12a from *Lachnospiraceae bacterium* (*Lb*Cas12a), which is frequently used in nucleic acid detection systems,[19,20] using single-molecule assay platform (Figure 1).[15] Given its recent public health relevance, Mpox virus (MPXV: dsDNA virus)[21] was selected as model target. For the single-molecule assay, a mixture of tgDNA, Cas12a−crRNA complexes, and FQ reporters was loaded into microchambers on a CD-based device and sealed with oil (Figure 1A). Under limiting-dilution conditions for tgDNA (e.g., 100 fM concentration), each chamber stochastically contains either zero or one activated (tgDNA-bound) Cas12a molecule. In chambers with an activated complex, the FQ reporters are

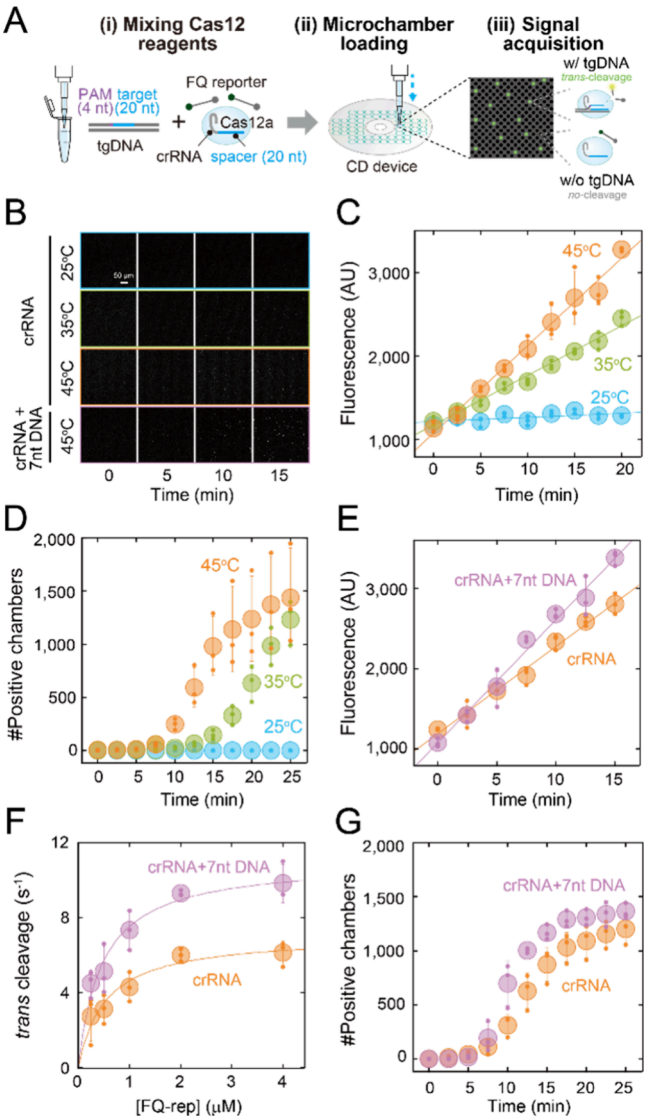


Figure 1. Single molecule analysis of Cas12a. (A) Schematics of single molecule analysis using microchamber arrays. (B) Representative fluorescence image in the presence of a 100 fM MPXV J2R gene fragment. (C, D) Time course of fluorescence increase (C) and number of fluorescence-positive chambers (D) at indicated temperatures. Representative traces are shown with error bars (standard deviation: SD). Solid lines indicate linear regressions. (E) Time course of fluorescence increase at 45 °C using crRNA without (orange) or with a 7-base DNA appending (purple). (F) *trans*-Cleavage rate measured at various concentrations of FQ reporters. The data were fitted to the Michaelis−Menten equation. (G) Time course of number of fluorescence-positive chambers. Error bars indicate the SD from three technical replicates.

trans-cleaved, leading to accumulation of fluorescent products. Consequently, fluorescence-positive chambers appeared discretely across the array (Figure 1B), and their fluorescence intensity increased linearly over time (Figure 1C), confirming single-molecule detection of Cas12a activity. Notably, the reaction chambers employed here have a volume of approximately 30 fL, which is approximately 2 orders of magnitude smaller than the picoliter-scale droplets (20−30 μm in diameter, corresponding to ∼4−14 pL) used in previously reported amplification-free single-molecule Cas12a detection systems.[22,23] Because the rate of fluorescent product

https://doi.org/10.1021/acs.analchem.6c00936
Anal. Chem. XXXX, XXX, XXX−XXX

accumulation per activated Cas12a molecule is inversely proportional to the reaction volume, our system achieves approximately 10^2-fold faster signal accumulation, enabling rapid detection and allowing detailed biophysical analysis of Cas12a *trans*-cleavage activity even under conditions where the activity is reduced (e.g., altered reaction conditions or in the presence of crRNA−target mismatches).

The *trans*-cleavage rate of *Lb*Cas12a was strongly temperature dependent (Figure 1C,D). The *trans*-cleavage rate of *Lb*Cas12a (6 s^{-1}, 2 μM reporter, 45 °C) was around 1/50 of those for Cas13a (~300 s^{-1}, 2 μM reporter, 25 °C[15]). Michaelis−Menten analysis of the *trans*-cleavage, performed by varying the FQ-reporter concentration, yielded V_{max} = 7.1 s^{-1} and K_m = 0.53 μM at 45 °C (Figure 1F and Figure S1). Activation efficiency of Cas12a was evaluated by counting chambers whose fluorescence exceeded a fixed threshold, termed positive chamber. The activation efficiency remained comparable at 35 and 45 °C (Figure 1D), implicating temperature as a regulator of *trans*-cleavage kinetics rather than activation efficiency in this temperature range. Subsequently, we investigated the effect of appending a 7-nt DNA (TATTATT) to the crRNA 3′ end using single-molecule analysis. A previous bulk biochemical study reported that such DNA appending enhanced Cas12a activity,[18] but it remained unclear whether this effect resulted from increased activation efficiency or elevated *trans*-cleavage rate. Accordingly, we separately quantified these parameters by the single-molecule analysis. It revealed that the DNA appending increased *trans*-cleavage rate (Figure 1E,F) while leaving activation efficiency unchanged (Figure 1G). Michaelis−Menten analysis showed that the V_{max} and K_m were 11.0 s^{-1} and 0.47 μM, respectively (Figure 1F). The ~1.6-fold increase in V_{max} with minimal change in K_m suggests that attaching DNA to the crRNA does not affect substrate binding; rather, it accelerates either the substrate *trans*-cleavage step or the release of the cleaved products. Under the condition, the number of positive chambers reached a plateau within approximately 15 min (Figure 1G), demonstrating the potential of Cas12a for rapid tgDNA detection.

tgDNA Recognition Specificity

*Lb*Cas12a recognizes a protospacer adjacent motif (PAM) of tgDNA with the canonical TTTV (V = A, C, or G) motif being optimal for target recognition and cleavage activity[19] (Figure 2A). In nucleic-acid detection applications, it is desirable to broaden the targetable sequence space by increasing the flexibility of PAM recognition. To this end, we engineered a variant of *Lb*Cas12a, termed en*Lb*Cas12a, by introducing mutations (D156R, G532R, and K538R) which were previously reported to enhance PAM recognition flexibility in Cas12a from *Acidaminococcus sp.*.[17]

Single-molecule analysis revealed that en*Lb*Cas12a shared comparable PAM preference profiles, while en*Lb*Cas12a produced, on average, 2.4-fold more positive chambers than *Lb*Cas12a (Figure 2B and Figure S3). Interestingly, the *trans*-cleavage rates were independent of the PAM sequences for both *Lb*Cas12a and en*Lb*Cas12a (Figure 2C and Figure S4). Consistent with this, Michaelis−Menten analysis showed that en*Lb*Cas12a displays kinetic parameters comparable to those of *Lb*Cas12a, with V_{max} and K_m values of 12.0 s^{-1} and 0.30 μM for the 7-nt DNA-appended crRNA (Figure S2). Together, these results indicate that PAM recognition primarily functions in initial binding to Cas12a−crRNA complex, leading to the

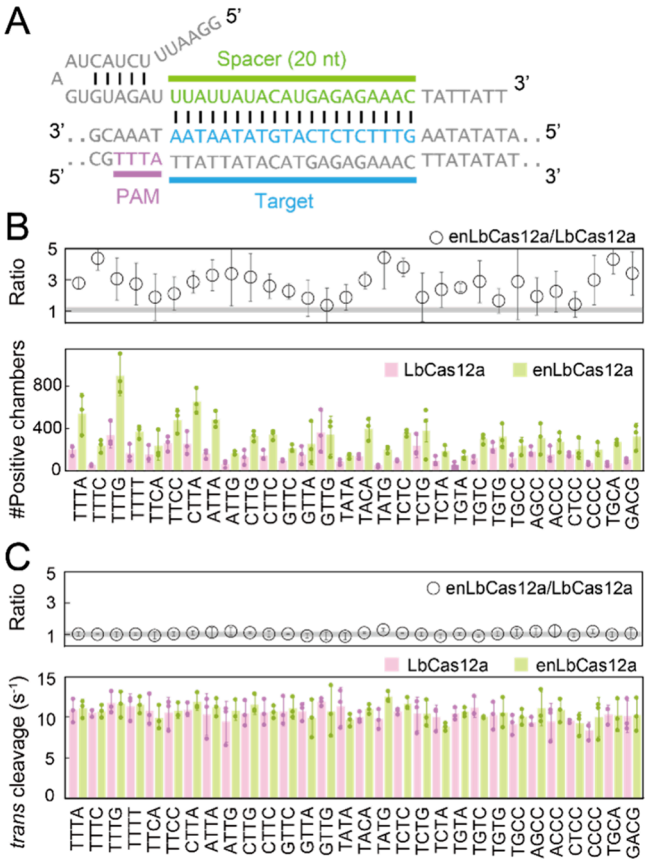


Figure 2. PAM-sequence dependence. (A) Sequence of crRNA and tgDNA. (B, C) Single-molecule analysis using tgDNAs bearing 30 different PAM sequences. The numbers of fluorescence-positive chambers (B) and *trans*-cleavage rate (C) were evaluated with 1 pM tgDNA at 45 °C for *Lb*Cas12a (pink) and en*Lb*Cas12a (green). Error bars indicate the SD from three technical replicates.

efficient structural transition responsible for *trans*-cleavage. Consequently, en*Lb*Cas12a combines enhanced sensitivity with an expanded targetable sequence range, making it well suited for nucleic acid detection applications.

Next, the effects of crRNA−tgDNA mismatches for en*Lb*Cas12a were systematically investigated by single-molecule analysis (Figure 3 and Figure S5). The *trans*-cleavage rates were found to be influenced by mismatches, and were particularly reduced by mismatches at positions 5, 9, and 10, causing a 2- to 4-fold decrease in activity (Figure 3B and Figure S5). Consistent with the reduced *trans*-cleavage rate, tgDNAs containing mismatches at these positions showed a drastic decrease in the number of positive chambers (Figure 3C). Furthermore, the introduction of double mismatches at these sites almost completely abolished *trans*-cleavage activity (Figure 3B and Figure S5), indicating a cooperative contribution of these positions to enzyme activation. One possible explanation for the reduction in *trans*-cleavage activity caused by these mismatches is that the conformational rearrangement required for catalytic activation is perturbed by local distortion of the crRNA−tgDNA hybrid. An AlphaFold 3 model of the en*Lb*Cas12a ternary complex (Figure S6) reveals that hybrid positions 9 and 10 are located adjacent to the RuvC-occluding "lid" loop (residues ~927−940).[24,25] Recent work has shown that the lid is maintained in an open, catalytically active conformation through allosteric

https://doi.org/10.1021/acs.analchem.6c00936
Anal. Chem. XXXX, XXX, XXX−XXX

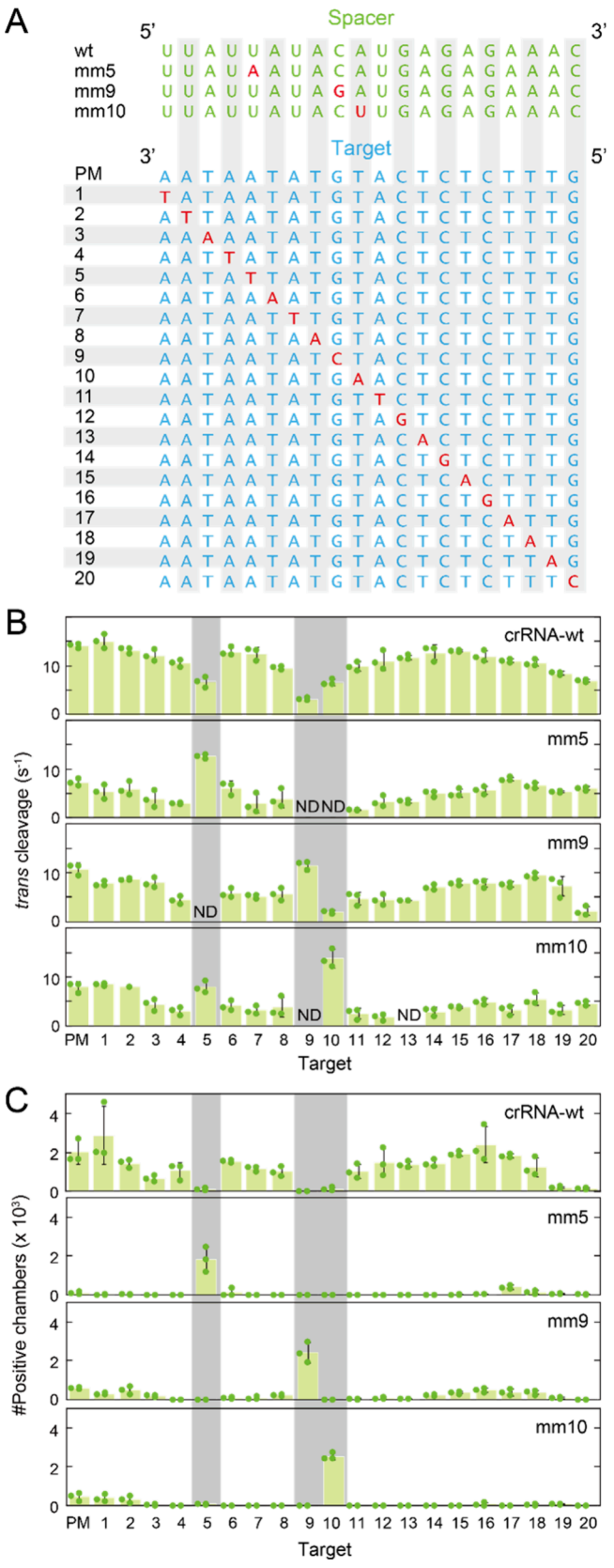


Figure 3. Mismatch dependence. (A) Sequences of crRNA and tgDNA. Mutations are highlighted in red. (B, C) Effects of mismatches on *trans*-cleavage rate (B) and the number of positive chambers (C) obtained with 1 pM tgDNAs. Values represent the mean ± SD (n = 3 technical replicates). PM and ND denote perfect matching and not detected, respectively.

coupling to the crRNA−tgDNA hybrid.[24] Local destabilization owing to the distorted hybrid at these positions would therefore weaken this coupling and shorten the lifetime of the catalytically competent open-lid state, providing a plausible structural basis for the observed position-dependent mismatch sensitivity.

Amplification-Free DNA Detection

We aimed to develop the en*Lb*Cas12a-based single-molecule platform for DNA virus diagnostics (Figure 4). A major limitation of the original system was the low capture efficiency of tgDNA in microchambers, as target molecules enter the chambers only stochastically through Brownian diffusion. To address this issue, we implemented a capture-enhancement approach using biotinylated Cas proteins and avidin-coated magnetic beads[15] (Figure 4A). In this approach, Cas12a−crRNA−tgDNA complexes are immobilized on magnetic

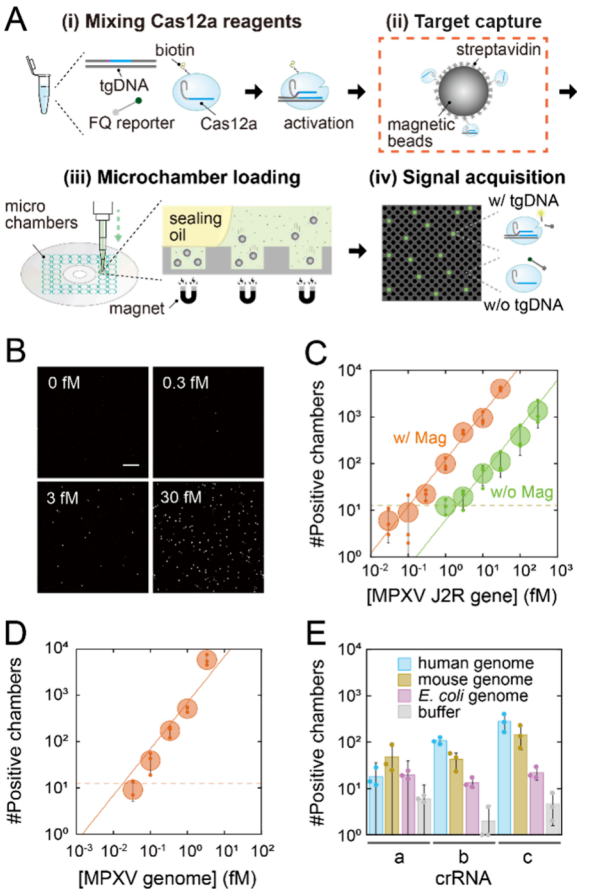


Figure 4. Amplification-free DNA detection for MPXV diagnosis. (A) Schematics of amplification-free DNA testing with a capture-enhancement approach. (B) Representative fluorescence image obtained at different concentrations of the MPXV J2R gene. The scale bar indicates 50 μm. (C) Number of positive chambers obtained at different concentrations of the MPXV J2R gene with (orange) or without a magnetic bead enrichment process (green). The solid lines indicate linear regressions. The values of the blank mean +3 SD are indicated by dotted lines (three technical replicates). (D) Number of positive chambers at different concentrations of the MPXV genome. (E) Cross-reactivity of en*Lb*Cas12a. The number of positive chambers was measured in the presence of 100 ng/mL genomic DNA derived from human, mouse, or *E. coli*. Three different crRNAs targeting distinct sequences in the MPXV gene were tested. Error bars indicate the SD from three technical replicates.

https://doi.org/10.1021/acs.analchem.6c00936
Anal. Chem. XXXX, XXX, XXX−XXX

beads via biotin−avidin interactions, after which the beads are actively concentrated into the microchambers under an external magnetic field. By circumventing diffusion-limited loading, this strategy markedly increases the per-chamber capture efficiency of Cas12a−crRNA−tgDNA complexes. Importantly, neither biotinylation, immobilization on magnetic beads, nor bead-derived autofluorescence significantly affected *trans*-cleavage activity or the identification of positive chambers (Figure S7), demonstrating that the enrichment strategy preserves both enzymatic activity and assay performance.

We then optimized the crRNA design for sensitive MPXV detection. The J2R gene, which encodes a TNFα receptor homologue, was selected as a target because it has been extensively validated as a diagnostic target in conventional real-time PCR assays, including the gold-standard assay established by the U.S. CDC.[26] Furthermore, because the J2R gene is located within the inverted terminal repeat (ITR) regions of the MPXV genome, it is present in two copies per viral genome, potentially providing a sensitivity advantage in single-molecule detection. Multiple crRNA candidates bearing the TTTA PAM preferred by en*Lb*Cas12a were designed and screened by single-molecule assays, and the one yielding the highest activation efficiency was selected as the optimal crRNA (Figure S8). Combining this optimal crRNA with the magnetic bead enrichment, we achieved highly sensitive detection of MPXV genes with a limit of detection (LoD) of 104 aM, representing a 20-fold improvement over the LoD obtained without the magnetic bead enrichment step (2.1 fM; Figure 4). The number of positive chambers increased as a function of MPXV gene concentration (Figure 4B,C), demonstrating the quantitative capability of this platform. This platform also successfully detected the full-length MPXV genome with a LoD of 18 aM (Figure 4D). The achieved sensitivity was comparable to that of the previous SATORI platform based on Cas13a for RNA detection. Notably, this attomolar sensitivity surpasses the picomolar fundamental limit reported for bulk amplification-free CRISPR-Cas12/Cas13 detection[12] by approximately 4 orders of magnitude, while matching the sensitivity of conventional real-time PCR within ∼15 min and without nucleic acid amplification.

Finally, we evaluated the potential cross-reactivity of the en*Lb*Cas12a-based platform against contaminating genomic DNAs. Despite the high mismatch discrimination in short (∼100 bp) target fragment assays as shown in Figure 3, we observed clear reactivity especially toward genomic DNA from human and mouse at 100 ng/mL (Figure 4E), indicating that nonspecific activation can occur in the presence of abundant background genomic DNAs. A genome-wide bioinformatic analysis identified on the order of 10^3 near-cognate sites per crRNA within four mismatches in the mammalian genomes (Table S5), suggesting that partial sequence complementarity at abundant near-cognate sites may contribute to the observed nonspecific activation. Notably, *Lb*Cas12a-K538R, a variant with more stringent PAM recognition,[27] also exhibited comparable nonspecific activation (Figure S9), indicating that this cross-reactivity is not unique to en*Lb*Cas12a.

To assess potential cross-reactivity under biologically relevant conditions, we further evaluated the assay in biological specimens using a direct single-molecule detection strategy recently established for blood samples.[14] Serum and nasopharyngeal swab samples from healthy donors produced substantial numbers of false-positive chambers (Figure S10). DNase treatment of the swab samples markedly reduced these false positives (Figure S10), indicating that endogenous genomic DNA is a major source of off-target enLbCas12a activation. These findings suggest that such cross-reactivity currently limits the direct application of the assay to clinical specimens. Consistent with previously reported off-target effects of Cas12a in genome editing,[28] our results identify a potential source of false-positive signals in amplification-free Cas12a-based diagnostics. Collectively, these findings underscore the need for Cas12a variants with improved target specificity and for systematic evaluation of cross-reactivity to enable reliable DNA virus detection in future applications.

CONCLUSIONS

Single-molecule analysis enabled a systematic biophysical characterization of Cas12a activity and identification of its optimal catalytic conditions. Compared with Cas13a,[15] Cas12a exhibited comparable activation efficiency; however, its *trans*-cleavage activity was >20-fold lower. For diagnostic applications, the current sensitivity appears sufficient, but the relatively low *trans*-cleavage activity limits the assay speed. In terms of target sequence discrimination, en*Lb*Cas12a demonstrated high specificity toward short DNA fragments but substantial nonspecific cross-reactivity with genome-length targets, underscoring the potential for false-positive outcomes in diagnostic settings.

The practical impact of this cross-reactivity, however, depends strongly on the detection format. In conventional Cas12a-based assays, preamplification of short DNA fragments confines target recognition to limited regions and sequence-specifically amplifies target-derived signals relative to off-target genomic signals, effectively suppressing cross-reactivity and false positive.[29] Even in bulk amplification-free Cas12a detection, the fundamental sensitivity is limited to the picomolar range,[12] such that contaminating genomic DNA at subpicomolar concentrations falls below the detection threshold and does not substantially affect the readout. In contrast, single-molecule amplification-free detection, as demonstrated in this work, reaches subfemtomolar sensitivity, at which even trace amounts of contaminating genomic DNA can generate detectable signals and lead to false positives. Indeed, Cas12a exhibited cross-reactivity with background DNAs, indicating that the risk of false positives cannot be easily avoided in this high-sensitivity, amplification-free regime. This challenge is expected to apply equally to other amplification-free single-molecule Cas12a-based detection formats, including droplet-based platforms,[23] which share the same underlying detection principle. Therefore, successful implementation of simple, single-molecule amplification-free DNA testing will likely require engineered Cas12a variants or the identification of orthologs with target specificity (and ideally also higher *trans*-cleavage activity) in the future.[30]

ASSOCIATED CONTENT

Supporting Information

The Supporting Information is available free of charge at https://pubs.acs.org/doi/10.1021/acs.analchem.6c00936.

Calibration curve of FAM-nucleotide; single-molecule analysis; screening of optimal crRNA; and lists of crRNA, tgDNA, and DNA templates/primers (PDF)

https://doi.org/10.1021/acs.analchem.6c00936
Anal. Chem. XXXX, XXX, XXX−XXX

AUTHOR INFORMATION

Corresponding Authors

Hajime Shinoda − *Molecular Physiology Laboratory, Pioneering Research Institute, RIKEN, Saitama 351-0198, Japan*; Email: hajime.shinoda@riken.jp

Rikiya Watanabe − *Molecular Physiology Laboratory, Pioneering Research Institute, RIKEN, Saitama 351-0198, Japan*; orcid.org/0000-0001-7146-2745; Email: rikiya.watanabe@riken.jp

Authors

Asami Makino − *Molecular Physiology Laboratory, Pioneering Research Institute, RIKEN, Saitama 351-0198, Japan*

Mami Yoshimura − *Molecular Physiology Laboratory, Pioneering Research Institute, RIKEN, Saitama 351-0198, Japan*

Tatsuya Iida − *Molecular Physiology Laboratory, Pioneering Research Institute, RIKEN, Saitama 351-0198, Japan*; orcid.org/0000-0003-0655-7937

Daisuke Yamazaki − *Molecular Physiology Laboratory, Pioneering Research Institute, RIKEN, Saitama 351-0198, Japan*

Noriko Minagawa − *Molecular Physiology Laboratory, Pioneering Research Institute, RIKEN, Saitama 351-0198, Japan*

Yasushi Kogo − *Molecular Physiology Laboratory, Pioneering Research Institute, RIKEN, Saitama 351-0198, Japan*

Takako Sano − *Kanagawa Prefectural Institute of Public Health, Kanagawa 253-0087, Japan*

Michio Jinnai − *Kanagawa Prefectural Institute of Public Health, Kanagawa 253-0087, Japan*

Takayuki Hishiki − *National Institute of Infectious Diseases, Japan Institute for Health Security, Tokyo 162-8640, Japan*

Hitomi Ohya − *Kanagawa Prefectural Institute of Public Health, Kanagawa 253-0087, Japan*

Hiroshi Nishimasu − *Research Center for Advanced Science and Technology, The University of Tokyo, Tokyo 153-8904, Japan; Department of Chemistry and Biotechnology, Graduate School of Engineering, The University of Tokyo, Tokyo 113-8656, Japan*

Complete contact information is available at: https://pubs.acs.org/10.1021/acs.analchem.6c00936

Author Contributions

H.S., H.N., and R.W. conceived and designed the experiments; H.S. and T.I. developed the assay platform; M.Y., N.M., Y.K., T.S., M.J., T.H., and H.O. prepared the sample; H.S. and A.M. performed the single-molecule assays; H.S., D.Y., and R.W. performed the data analysis. H.S. and R.W. wrote the manuscript.

Notes

The authors declare no competing financial interest.

ACKNOWLEDGMENTS

We thank all members of the Watanabe Laboratory for helpful discussions and comments, and Dr. Ryoya Nakagawa for sample preparation. This work was supported by JST CREST (JPMJCR19H5), AMED (JP21fk0108423h0001, JP22fk0108505h0001), BRIDGE (Cabinet Office, Government of Japan) to R.W.

REFERENCES

(1) Khan, S. F.; Rathod, P.; Gupta, V. K.; Khedekar, P. B.; Chikhale, R. V. Evolution and Impact of Nucleic Acid Amplification Test (NAAT) for Diagnosis of Coronavirus Disease. *Anal. Chem.* **2024**, *96* (20), 8124−8146.

(2) Kevadiya, B. D.; Machhi, J.; Herskovitz, J.; Oleynikov, M. D.; Blomberg, W. R.; Bajwa, N.; Soni, D.; Das, S.; Hasan, M.; Patel, M.; et al. Diagnostics for SARS-CoV-2 infections. *Nat. Mater.* **2021**, *20* (5), 593−605.

(3) Weng, Z.; You, Z.; Yang, J.; Mohammad, N.; Lin, M.; Wei, Q.; Gao, X.; Zhang, Y. CRISPR-Cas Biochemistry and CRISPR-Based Molecular Diagnostics. *Angew. Chem., Int. Ed. Engl.* **2023**, *62* (17), No. e202214987.

(4) Gootenberg, J. S.; Abudayyeh, O. O.; Lee, J. W.; Essletzbichler, P.; Dy, A. J.; Joung, J.; Verdine, V.; Donghia, N.; Daringer, N. M.; Freije, C. A.; et al. Nucleic acid detection with CRISPR-Cas13a/C2c2. *Science* **2017**, *356* (6336), 438−442.

(5) Chen, J. S.; Ma, E.; Harrington, L. B.; Da Costa, M.; Tian, X.; Palefsky, J. M.; Doudna, J. A. CRISPR-Cas12a target binding unleashes indiscriminate single-stranded DNase activity. *Science* **2018**, *360* (6387), 436−439.

(6) Makarova, K. S.; Wolf, Y. I.; Iranzo, J.; Shmakov, S. A.; Alkhnbashi, O. S.; Brouns, S. J. J.; Charpentier, E.; Cheng, D.; Haft, D. H.; Horvath, P.; et al. Evolutionary classification of CRISPR-Cas systems: a burst of class 2 and derived variants. *Nat. Rev. Microbiol* **2020**, *18* (2), 67−83.

(7) Tang, Y.; Gao, L.; Feng, W.; Guo, C.; Yang, Q.; Li, F.; Le, X. C. The CRISPR-Cas toolbox for analytical and diagnostic assay development. *Chem. Soc. Rev.* **2021**, *50* (21), 11844−11869.

(8) Kellner, M. J.; Koob, J. G.; Gootenberg, J. S.; Abudayyeh, O. O.; Zhang, F. SHERLOCK: nucleic acid detection with CRISPR nucleases. *Nat. Protoc* **2019**, *14* (10), 2986−3012.

(9) Ando, J.; Watanabe, R. Toward versatile digital bioanalysis. *Biomicrofluidics* **2023**, *17* (6), No. 061303.

(10) Talebian, S.; Dehghani, F.; Weiss, P. S.; Conde, J. Evolution of CRISPR-enabled biosensors for amplification-free nucleic acid detection. *Trends Biotechnol* **2024**, *42* (1), 10−13.

(11) Xia, Y.; Rao, R.; Xiong, M.; He, B.; Zheng, B.; Jia, Y.; Li, Y.; Yang, Y. CRISPR-Powered Strategies for Amplification-Free Diagnostics of Infectious Diseases. *Anal. Chem.* **2024**, *96* (20), 8091−8108.

(12) Huyke, D. A.; Ramachandran, A.; Bashkirov, V. I.; Kotseroglou, E. K.; Kotseroglou, T.; Santiago, J. G. Enzyme Kinetics and Detector Sensitivity Determine Limits of Detection of Amplification-Free CRISPR-Cas12 and CRISPR-Cas13 Diagnostics. *Anal. Chem.* **2022**, *94* (27), 9826−9834.

(13) Ueda, T.; Shinoda, H.; Makino, A.; Yoshimura, M.; Iida, T.; Watanabe, R. Purification/Amplification-Free RNA Detection Platform for Rapid and Multiplex Diagnosis of Plant Viral Infections. *Anal. Chem.* **2023**, *95* (25), 9680−9686.

(14) Furukawa, R.; Shinoda, H.; Tozaki, T.; Makino, A.; Yoshimura, M.; Iida, T.; Kawate, K.; Kikuchi, M.; Ishige, T.; Takahashi, Y.; et al. Direct Single-Molecule Detection of mRNA-LNP Drugs in Blood. *Anal. Chem.* **2026**, *98*, 756.

(15) Shinoda, H.; Iida, T.; Makino, A.; Yoshimura, M.; Ishikawa, J.; Ando, J.; Murai, K.; Sugiyama, K.; Muramoto, Y.; Nakano, M.; et al. Automated amplification-free digital RNA detection platform for rapid and sensitive SARS-CoV-2 diagnosis. *Commun. Biol.* **2022**, *5* (1), 473.

(16) Shinoda, H.; Taguchi, Y.; Nakagawa, R.; Makino, A.; Okazaki, S.; Nakano, M.; Muramoto, Y.; Takahashi, C.; Takahashi, I.; Ando, J.; et al. Amplification-free RNA detection with CRISPR-Cas13. *Commun. Biol.* **2021**, *4* (1), 476.

(17) Kleinstiver, B. P.; Sousa, A. A.; Walton, R. T.; Tak, Y. E.; Hsu, J. Y.; Clement, K.; Welch, M. M.; Horng, J. E.; Malagon-Lopez, J.; Scarfo, I.; et al. Engineered CRISPR-Cas12a variants with increased activities and improved targeting ranges for gene, epigenetic and base editing. *Nat. Biotechnol.* **2019**, *37* (3), 276−282.

(18) Nguyen, L. T.; Smith, B. M.; Jain, P. K. Enhancement of trans-cleavage activity of Cas12a with engineered crRNA enables amplified nucleic acid detection. *Nat. Commun.* **2020**, *11* (1), 4906.
(19) Yamano, T.; Zetsche, B.; Ishitani, R.; Zhang, F.; Nishimasu, H.; Nureki, O. Structural Basis for the Canonical and Non-canonical PAM Recognition by CRISPR-Cpf1. *Mol. Cell* **2017**, *67* (4), 633−645.
(20) Zetsche, B.; Gootenberg, J. S.; Abudayyeh, O. O.; Slaymaker, I. M.; Makarova, K. S.; Essletzbichler, P.; Volz, S. E.; Joung, J.; van der Oost, J.; Regev, A.; et al. Cpf1 is a single RNA-guided endonuclease of a class 2 CRISPR-Cas system. *Cell* **2015**, *163* (3), 759−771.
(21) Sanchez Clemente, N.; Coles, C.; Paixao, E. S.; Brickley, E. B.; Whittaker, E.; Alfven, T.; Rulisa, S.; Agudelo Higuita, N.; Torpiano, P.; Agravat, P.; et al. Paediatric, maternal, and congenital mpox: a systematic review and meta-analysis. *Lancet Glob Health* **2024**, *12* (4), e572−e588.
(22) Yue, H.; Shu, B.; Tian, T.; Xiong, E.; Huang, M.; Zhu, D.; Sun, J.; Liu, Q.; Wang, S.; Li, Y.; et al. Droplet Cas12a Assay Enables DNA Quantification from Unamplified Samples at the Single-Molecule Level. *Nano Lett.* **2021**, *21* (11), 4643−4653.
(23) Zhang, Y.; Liu, H.; Tang, S.; Yalikun, Y.; Barber, T.; Goda, K.; Li, M. Double-emulsion droplet digital CRISPR/Cas12a for amplification-free, absolute quantification of nucleic acids at attomole levels. *Chem. Eng. J.* **2025**, *512*, No. 162098.
(24) Newman, A.; Starrs, L.; Burgio, G. Nuc domain electrostatics drive the trans cleavage activity of CRISPR-Cas12a. *Nucleic Acids Res.* **2026**, *54* (1), No. gkaf1485.
(25) Saha, A.; Ahsan, M.; Arantes, P.; Schmitz, M.; Chanez, C.; Jinek, M.; Palermo, G. An alpha-helical lid guides the target DNA toward catalysis in CRISPR-Cas12a. *Nat. Commun.* **2024**, *15* (1), 1473.
(26) Li, Y.; Zhao, H.; Wilkins, K.; Hughes, C.; Damon, I. K. Real-time PCR assays for the specific detection of monkeypox virus West African and Congo Basin strain DNA. *J. Virol Methods* **2010**, *169* (1), 223−227.
(27) Zhou, J.; Chen, P.; Wang, H.; Liu, H.; Li, Y.; Zhang, Y.; Wu, Y.; Paek, C.; Sun, Z.; Lei, J.; et al. Cas12a variants designed for lower genome-wide off-target effect through stringent PAM recognition. *Mol. Ther* **2022**, *30* (1), 244−255.
(28) Kim, D.; Luk, K.; Wolfe, S. A.; Kim, J. S. Evaluating and Enhancing Target Specificity of Gene-Editing Nucleases and Deaminases. *Annu. Rev. Biochem.* **2019**, *88*, 191−220.
(29) Kaminski, M. M.; Abudayyeh, O. O.; Gootenberg, J. S.; Zhang, F.; Collins, J. J. CRISPR-based diagnostics. *Nat. Biomed Eng.* **2021**, *5* (7), 643−656.
(30) Kim, H.; Lee, W. J.; Oh, Y.; Kang, S. H.; Hur, J. K.; Lee, H.; Song, W.; Lim, K. S.; Park, Y. H.; Song, B. S.; et al. Enhancement of target specificity of CRISPR-Cas12a by using a chimeric DNA-RNA guide. *Nucleic Acids Res.* **2020**, *48* (15), 8601−8616.



https://doi.org/10.1021/acs.analchem.6c00936
Anal. Chem. XXXX, XXX, XXX−XXX